Polymers **2015**, *7*, 896-908; doi:10.3390/polym7050896

OPEN ACCESS

polymers

ISSN 2073-4360

www.mdpi.com/journal/polymers

Article

Synthesis and Characterization of [60]Fullerene-Glycidyl Azide Polymer and Its Thermal Decomposition

Ting Huang [1], Bo Jin [1,2,*], Ru Fang Peng [1,*], Cong Di Chen [1], Rong Zong Zheng [1], Yi He [2] and Shi Jin Chu [1]

[1] State Key Laboratory Cultivation Base for Nonmetal Composites and Functional Materials, Southwest University of Science and Technology, Mianyang 621010, Sichuan, China; E-Mails: huangting9007@163.com (T.H.); smileccd@sina.cn (C.D.C.); iozz123@163.com (R.Z.Z.); chushijin@swust.edu.cn (S.J.C.)

[2] School of National Defence Science and Technology, Southwest University of Science and Technology, Mianyang 621010, Sichuan, China; E-Mail: heyi@swust.edu.cn

* Authors to whom correspondence should be addressed; E-Mails: jinbo@swust.edu.cn (B.J.); pengrufang@swust.edu.cn (R.F.P.); Tel./Fax: +86-816-2419011 (B.J.).

Academic Editor: Alexander Böker

Received: 26 February 2015 / Accepted: 20 April 2015/ Published: 5 May 2015

Abstract: A new functionalized [60]fullerene-glycidyl azide polymer (C_{60}-GAP) was synthesized for the first time using a modified Bingel reaction of [60]fullerene (C_{60}) and bromomalonic acid glycidyl azide polymer ester (BM-GAP). The product was characterized by Fourier transform infrared (FTIR), ultraviolet-visible (UV-Vis), and nuclear magnetic resonance spectroscopy (NMR) analyses. Results confirmed the successful preparation of C_{60}-GAP. Moreover, the thermal decomposition of C_{60}-GAP was analyzed by differential scanning calorimetry (DSC), thermogravimetric analysis coupled with infrared spectroscopy (TGA-IR), and *in situ* FTIR. C_{60}-GAP decomposition showed a three-step thermal process. The first step was due to the reaction of the azide group and fullerene at approximately 150 °C. The second step was ascribed to the remainder decomposition of the GAP main chain and *N*-heterocyclic at approximately 240 °C. The final step was attributed to the burning decomposition of amorphous carbon and carbon cage at around 600 °C.

Keywords: C_{60}; glycidyl azide polymer (GAP); thermal analysis; energetic material

1. Introduction

Fullerene has been extensively developed with remarkable achievement since Kratschmer *et al.* first produced [60]fullerene (C_{60}) on a preparative scale [1,2]. C_{60} and its functionalized derivatives are important and can be remarkably applied in various studies because of their unique structure and physical properties [3–5]. As C_{60} has good features such as thermal stability, antioxidation, etching resistance, good compatibility with propellant components, and beneficial for preventing aging [6], C_{60} can replace carbon black as the solid rocket fuel additive that can increase the burning rate and combustion catalytic efficiency and decrease the amount of NO_x in the exhaust gas [7,8]. If some energetic groups, such as the nitro group, would be added into C_{60}, an enhanced fuel additive may be obtained [9]. Numerous nitration methods have been used to synthesize polynitro-fullerene derivatives under different conditions and nitration reagents, such as nitric acid [10], NO_2 [11–13], or N_2O_4 [14], in CS_2. Generally, the nitro group that directly bonds to fullerene reacts slowly with H_2O to afford partially hydroxylated products poly(hydroxynitro)-fullerenes [13]. Therefore, achieving a stable energetic fullerene derivative remains a challenge.

Energetic polymers with azide groups have recently attracted much attention, because they can be used in solid rocket propellant systems and composite explosives as plasticizers to reduce the vulnerability of storage and transport, impart additional energy, increase performance, improve mechanical properties, and enhance system stability [15–17]. Moreover, the terminal hydroxyl group of glycidyl azide polymer (GAP) can be easily modified through various reactions such as esterification, acetalization, etherification, *etc.* [18–24]. In this paper, GAP was further functionalized via esterification with malonyl dichloride and subsequent brominate reaction to afford bromomalonic acid GAP ester (BM-GAP), which can easily react with C_{60} through a modified Bingel reaction [25] to afford a new fullerene derivative, namely, [60]fullerene GAP (C_{60}-GAP), which perhaps could become a new material of energetic burning rate additive. The thermal decomposition performance and decomposition mechanism of C_{60}-GAP were also examined in detail.

2. Experimental Section

2.1. Materials and Methods

The reagents for the organic synthesis were pure commercial products from Aladdin Industrial Corporation (Shanghai, China). The solvents were purchased from Kelong Chemical Reagents Co. (Chengdu, China). The 300–400 mesh silica gel was purchased from Qingdao Hailang. GAP (M_n = 505, M_w/M_n = 1.39) were provided by the Liming Chemical Engineering Research and Design Institute of Luoyang. C_{60} was obtained from Puyang Yongxin Fullerene Technology Co., Ltd. (purity > 99.5%). All the chemicals were used as received.

2.2. Synthesis of Malonic Acid Glycidyl Azide Polymer Ester

Malonyl chloride (1.25 mL, 13 mmol) diluted with 30 mL of CH_2Cl_2 were added dropwise to a stirred solution of GAP (M_n = 505, M_w/M_n = 1.39) (10 g, 26 mmol) and *N*,*N*-dimethylformamide (0.76 mL, 13 mmol) as acid binding agent in redistilled CH_2Cl_2 (100 mL) under N_2 atmosphere in an

ice bath. The mixture was stirred for 30 min and then overnight at room temperature. The reaction solution was repeatedly washed with deionized water to neutralize the pH. The organic phase was collected and dried by anhydrous Na_2SO_4. After filtration, the solution was dried at 45 °C in vacuum to achieve 9.34 g (yield of 86%) of malonic acid glycidyl azide polymer ester (M-GAP). The GPC analysis revealed a molecular weight (M_n) of 1197 g/mol and a molecular weight distribution (M_w/M_n) of 1.31. ^{1}H NMR (400 MHz, $CDCl_3$, δ): 5.12 (br, 2H, CH_2), 3.77–3.48 (m, 3H, CH_2CH), 3.45–3.30 (m, 2H, CH_2N_3), 1.29–1.12 (m, 3H, C*H*$_3$); FT-IR (KBr): υ = 2929 (–CH–), 2876 (–CH_2–), 2102, 1280 (–N_3), 1756, 1739 (C=O), 1118 (C–O–C), 986, 936, 849, 670, 628, 556 cm^{-1}.

2.3. Synthesis of Bromomalonic Acid Glycidyl Azide Polymer Ester

Bromine (0.31 mL) diluted in 10 mL of CH_2C1_2 was slowly dropped in a stirred solution of 4.67 g M-GAP in 100 mL CH_2C1_2, and the mixture was stirred at 30 °C for 30 min. The mixture color gradually changed from yellow to orange-red after bromine was added dropwise to the mixture, and after 6 h of stirring, the solution color became stable. The resulting solution was repeatedly washed by saturated NaBr solution and deionized water to neutralize the solution. The organic phase was dried with anhydrous Na_2SO_4. After filtration, the filtrate was rotary evaporated to remove the solvent and dried under 45 °C in vacuum to yield 4.36 g (yield of 85%) of bromomalonic acid glycidyl azide polymer ester (BM-GAP). The GPC analysis revealed a molecular weight (M_n) of 1268 g/mol and a molecular weight distribution (M_w/M_n) of 1.36. ^{1}H NMR (400 MHz, $CDCl_3$, δ): 5.13 (s, 1H, CHBr), 3.76–3.46 (m, 3H, CH_2CH), 3.43–3.26 (m, 2H, CH_2N_3), 1.25–1.11 (m, 3H, CH_3); FT-IR (KBr): *υ*= 2929 (–CH–), 2876 (–CH_2–), 2100, 1279 (–N_3), 1755, 1746 (C=O), 1115 (C–O–C), 989, 936, 850, 671, 630, 556 cm^{-1}.

2.4. Synthesis of [60]Fullerene Glycidyl Azide Polymer

0.1198 g C_{60} (0.17 mmol) and 0.1066 g glycine (0.17 mmol) were dissolved in 100 mL of chlorobenzene and 30 mL of DMSO by using ultrasonic irradiation method. Thereafter, 0.6755 g of BM-GAP was added to the above solution under mild stirring. The mixture was stirred at room temperature for 12 h, and then the resulting solution was repeatedly washed with deionized water to remove DMSO and sarcosine. Chlorobenzene was then removed under vacuum. The residue was separated on a silica gel column with carbon disulfide as the eluent to obtain 23.50 mg unreacted C_{60} and with toluene/ethyl acetate (1:2) as the eluent to afford the crude product of C_{60}-GAP. Then the crude product was washed with 150 mL methanol (3 × 50 mL) and dried *in vacuo* at 50 °C to afford 0.3048 g C_{60}-GAP, with a yield of 83%. The GPC analysis revealed a molecular weight (M_n) of 2176 g/mol and a molecular weight distribution (M_w/M_n) of 1.45. ^{1}H NMR (400 MHz, $CDCl_3$, δ): 3.74–3.43 (m, 3H, CH_2CH), 3.41–3.24 (m, 2H, CH_2N_3), 1.21–1.09 (m, 3H, CH_3); FT-IR (KBr): *υ* = 2920 (–CH–), 2867 (–CH_2–), 2198 (–N_3), 1744 (C=O), 1110 (C–O–C), 524, 1219,1456 (C_{60}), 945, 872, 663, 590 cm^{-1}.

2.5. Characterization

FTIR spectra were recorded on a Nicolet 6700 FTIR spectrometer (Thermo Fisher Scientific Co., Waltham, MA, USA) with a resolution of 4 cm^{-1} from 400 to 4000 cm^{-1} wavelength by being pressed with KBr tablet. UV-Vis spectra were collected on a UNICON UV-2102 PCS spectrometer (Shimadzu Co., Kyoto, Japan) with a rate of 1 nm/min from 200 to 600 nm wavelength and dichloromethane as solvent. ^{1}H NMR and ^{13}C NMR spectra were recorded at room temperature on a Bruker Advance DRX 400-MHz instrument (Bruker BioSpin AG, Fällanden, Switzerland) with $CDCl_3$ as the solvent and tetramethylsilane as internal standard. Gel permeation chromatography (GPC) was recorded on preplinc GPC spectrometer (J2 Scientific Co., Columbia, MO, USA) with an injection volume of 10 mL and tetrahydrofuran (THF) as the solvent. Differential scanning calorimetry (DSC) experiment was obtained in the 0–500 °C temperature range on a Q200 DSC instrument (TA Instruments Co., New Castle, DE, USA) at a heating rate of 10 °C/min under high-purity nitrogen flow (99.99%; flow rate, 50 mL/min). Thermogravimetry analysis (TGA) was performed in the 0–800 °C temperature range on a SDT Q600 TGA instrument (TA Instruments Co., New Castle, DE, USA) in air atmosphere with a heating rate of 10 °C/min.

3. Results and Discussion

3.1. Synthesis and Characterization of C_{60}-GAP

C_{60} can replace carbon black as the solid rocket fuel additive that can increase the burning rate and combustion catalytic efficiency, but both C_{60} and carbon black are the inert catalyst, and adding C_{60} or carbon black into propellant will reduce the energy of propellant [8]. Therefore, obtaining a stable energetic fullerene derivative remains a challenge. Considering glycidyl azide polymer (GAP) is an azide energetic material and can be easily modified through various reactions, GAP was grafted on C_{60} to afford energetic fullerene derivatives C_{60}-PGN in three steps, as shown in Scheme 1. Firstly, M-GAP was synthesized through esterification of monomethyl-terminated GAP and malonyl chloride. Then, M-GAP was brominated using bromine as brominating agent and the bromosubstituted product BM-GAP was obtained. Subsequently, BM-GAP reacted with C_{60} through a modified Bingel reaction [25] to yield C_{60}-GAP.

The C_{60}-GAP structure was characterized by UV-vis, FTIR, and ^{1}H and ^{13}C NMR spectroscopy analyses. Figure 1 shows the FTIR spectrum of C_{60}-GAP. The peaks located at 524, 1219, and 1456 cm^{-1} are the characteristic absorption peaks of C_{60}, and the strong absorption peak at 2098 cm^{-1} corresponds to the $–N_3$ group of GAP. The peaks at 2920 and 2867 cm^{-1} are ascribed to the C–H symmetric and antisymmetric stretching vibrations of GAP, respectively. The broad intense stretching vibration absorption peak at 1110 cm^{-1} is attributed to the ester group C–O–C stretching vibration. In addition, a strong absorption band at 1744 cm^{-1} clearly indicates the carbonyl group (C=O) stretching vibration of the ester group [26].

The UV-Vis spectra of C_{60}, BM-GAP, and C_{60}-GAP are shown in Figure 2. The C_{60} UV-Vis spectrum shows the cage absorption peaks at approximately 231, 258, 331, and 405 nm. The BM-GAP UV-Vis spectrum shows an absorption peak at 296 nm. Compared with BM-GAP, three absorption peaks at 285, 314, and 427 nm appear in the C_{60}-GAP UV-Vis spectrum, which shows the GAP group

in C_{60}, and the weak absorption band at 427 nm is typical of monoadducts at the closed 6,6-junction of C_{60} [27].

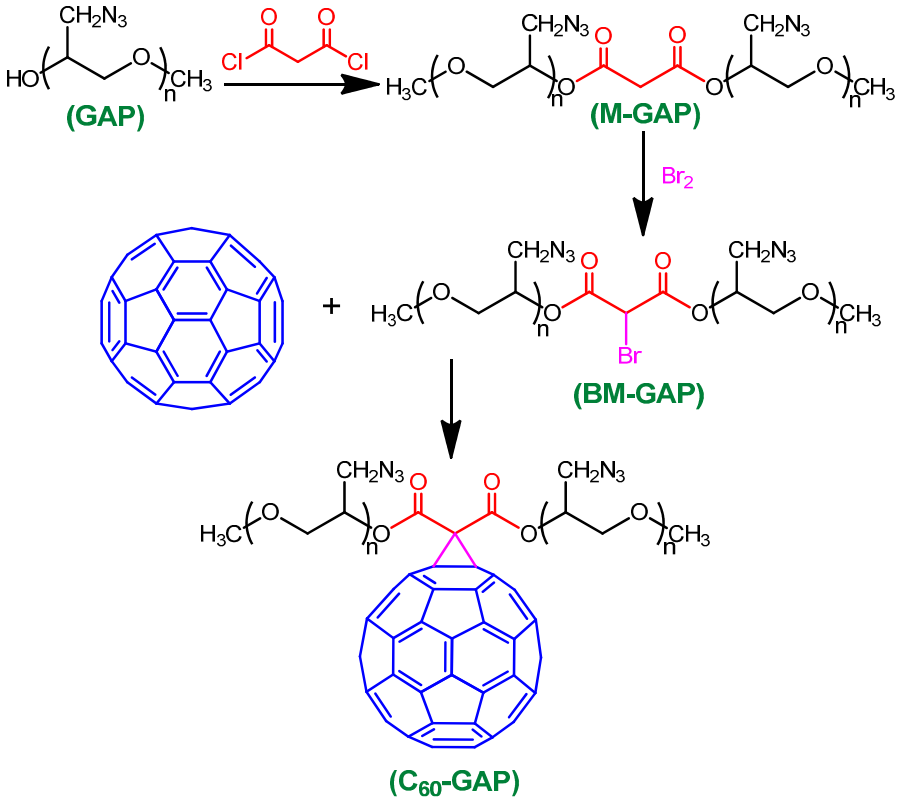

Scheme 1. Schematic representation of [60]fullerene-glycidyl azide polymer (C_{60}-GAP) synthesis.

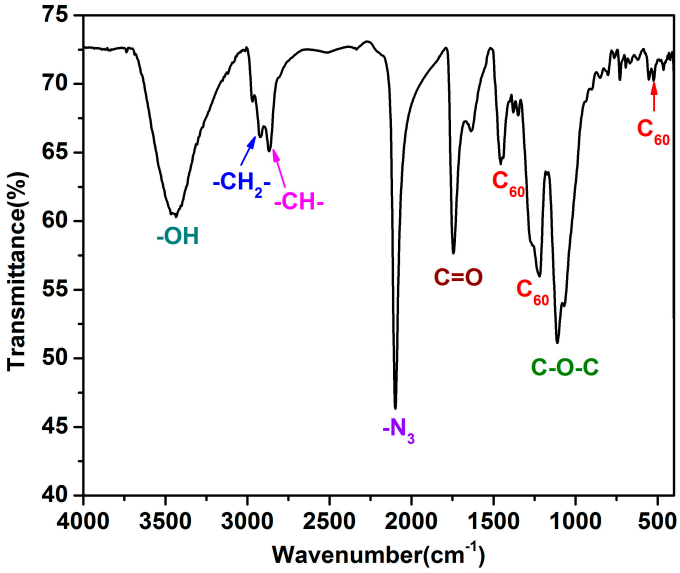

Figure 1. Fourier transform infrared (FTIR) spectrum of C_{60}-GAP.

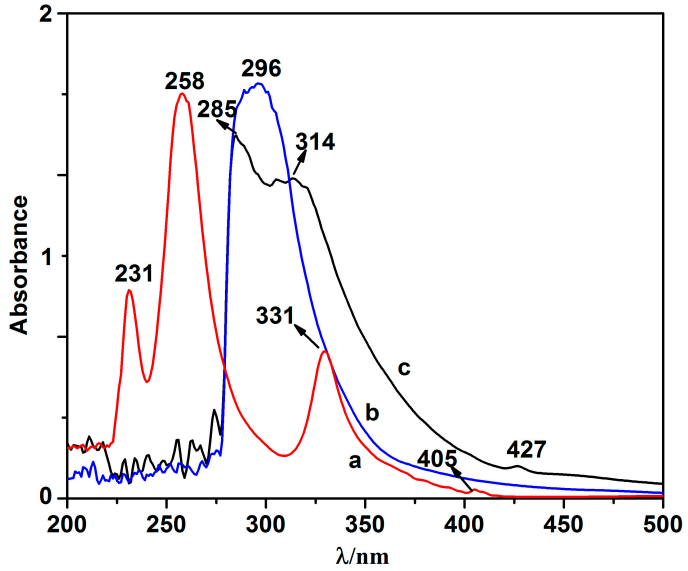

Figure 2. UV-Vis spectra of (**a**) C_{60}, (**b**) bromomalonic acid glycidyl azide polymer ester (BM-GAP) and (**c**) C_{60}-GAP.

Figure 3a,b represent the ^{1}H NMR spectra of BM-GAP and C_{60}-GAP, respectively. In Figure 3a, the peaks at around 3.76 and 3.45 ppm are attributed to three –CH_2CH– protons (denoted b and c) of the polyether main chain of GAP, respectively. The peaks from 3.43 to 3.26 ppm are attributed to two –CH_2N_3 protons (denoted d) of the pendant group of GAP, and the peaks observed from 1.25 to 1.11 ppm are ascribed to the three methyl-terminated protons (–CH_3, denoted a) [28]. An evident peak at 5.13 ppm belongs to the –CHBr– proton (denoted e). In Figure 3b, the ^{1}H NMR spectrum of C_{60}-GAP is similar to that of BM-GAP, but lower signal less at approximately 5.13 ppm and the chemical shift of each proton moves upfield because of the reaction with C_{60}.

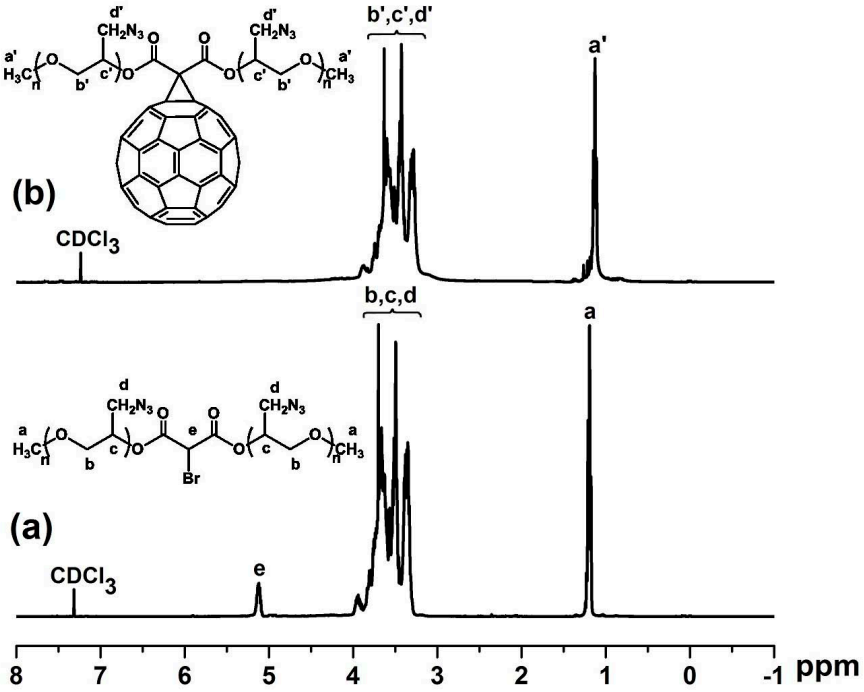

Figure 3. ^{1}H NMR spectra of (**a**) BM-GAP and (**b**) C_{60}-GAP.

The ^{13}C NMR spectra of BM-GAP and C_{60}-GAP are presented in Figure 4. In Figure 4a, the brominated active methylene carbon (–COCHBrCO–, denoted a) of BM-GAP appears at approximately 50.52 ppm. The signals from 52.12 to 51.34 ppm are attributed to the azidomethyl carbon of azidoacetate group (–$CH_2CH(CH_2N_3)$O–, denoted d). The peaks around 70.17 to 69.31 ppm result from the methylene carbon of the main chain (–$CH_2CH(CH_2N_3)$O–, denoted e). The peaks at approximately 79.57 to 78.43 ppm are attributed to the methine carbon of the main chain (–$CH_2CH(CH_2N_3)$O–, denoted c) [27], and the peak at 68.19 ppm is attributed to the methyl-terminated carbon (–OCH_3, denoted f) [29]. The carbonyl carbon (C=O, denoted b) of the main chain appears at around 165.58 ppm [30]. When BM-GAP reacts with C_{60}, the chemical shift of each carbon for C_{60}-GAP (Figure 4b) moves upfield. In Figure 4b, the two sp^3-carbons of the C_{60} cage (denoted g') appear at 73.34 ppm, and 58 sp^2-carbons of fullerene cage (denoted h') overlap and appear from 153.31 to 130.34 ppm as a broad peak [31,32].

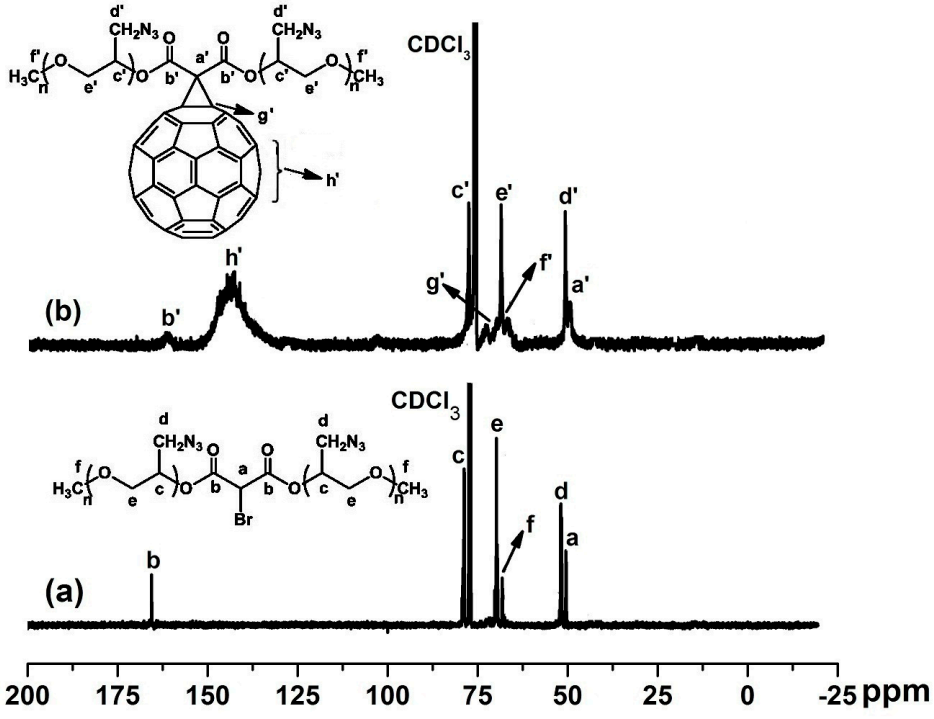

Figure 4. ^{13}C NMR spectra of (**a**) BM-GAP and (**b**) C_{60}-GAP.

3.2. Thermal Analysis

The thermal stability of energetic materials has an important effect on the preparation, storage, processing, and application properties of these materials. Thus, DSC and TGA methods were adopted to evaluate the decomposition behavior of C_{60}-GAP.

The DSC curve of C_{60}-GAP under N_2 atmosphere is shown in Figure 5. Only two exothermic peaks for C_{60}-GAP appear from 100 to 500 °C. The first exothermic peak at 155 °C is probably caused by the initial intramolecular or intermolecular cycloaddition of the $–N_3$ group and fullerene carbon cage and subsequent decomposition to release nitrogen [33–37]. The other exothermic peak at 242 °C is maybe due to the GAP main chain and *N*-heterocyclic decomposition.

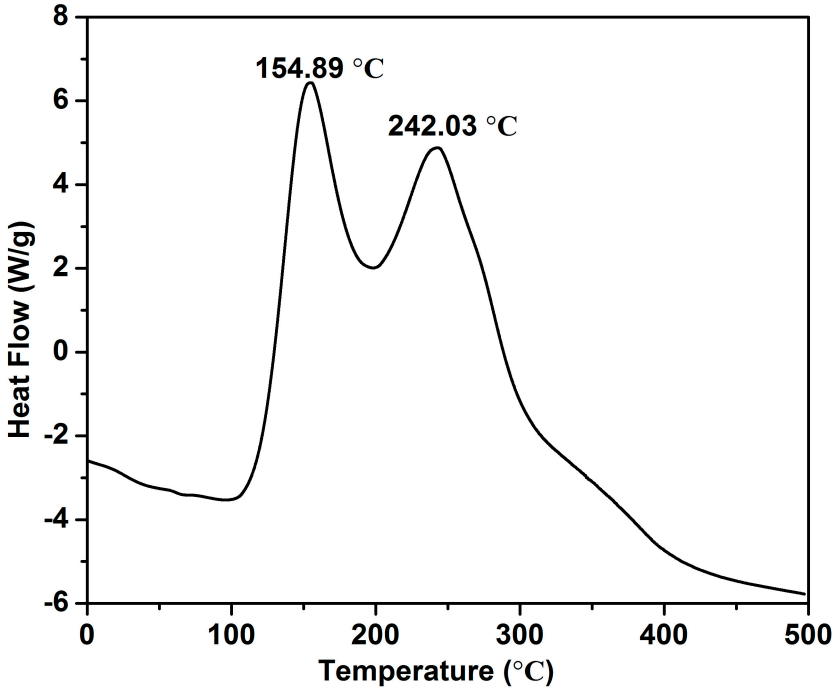

Figure 5. Differential scanning calorimetry (DSC) curve of C_{60}-GAP under N_2 atmosphere.

TGA-IR spectroscopy was used to rapidly identify the constituents of the thermal decomposition gas to determine the thermal decomposition mechanism of C_{60}-GAP (Figure 6). In Figure 6a, the TGA curve shows the three-step thermal degradation of C_{60}-GAP under air atmosphere. The first stage of thermal degradation appears at 150 °C, with around 10.35% weight loss. The other two onsets thermal degradations appear at 300 °C and 600 °C, with approximately 22.89% and 64.18% weight losses, respectively. Figure 6c,d depict the IR spectra of the gas phase products of thermal decomposition of C_{60}-GAP at 300 and 580 °C, respectively. In Figure 6c, the decomposed products of C_{60}-GAP at 300 °C under air atmosphere are mainly CO_2 (2306 and 2348 cm^{-1}), NO (1829 cm^{-1}), NO_2 (1635 cm^{-1}), and H_2O (3448 cm^{-1} and 1400–1600 cm^{-1}). Figure 6d shows that the decomposed products of C_{60}-GAP at 580 °C under air atmosphere are mainly CO_2 (2306, 2333, 2358, and 2377 cm^{-1}), CO (2109 and 2176 cm^{-1}), and H_2O (3452 cm^{-1} and 1400–1600 cm^{-1}). By contrast, the decomposition temperature of GAP is at approximately 200 °C, and the main gas products are CO, HCN, HCHO, and NH_3 [38–40]. Thus, the results indicate that the first thermal degradation of C_{60}-GAP at 150 °C is probably due to the decomposition of the $–N_3$ group, and the decomposition of $–N_3$ at 150 °C is probably going through the initial intramolecular or intermolecular cycloaddition of $–N_3$ and fullerene carbon cage and subsequent decomposition to release nitrogen. The second thermal degradation at about 200~400 °C is probably due to the decomposition of the GAP main chain and *N*-heterocyclic decomposition; and the last step is maybe because of the thermal decomposition of fullerene cage (Scheme 2).

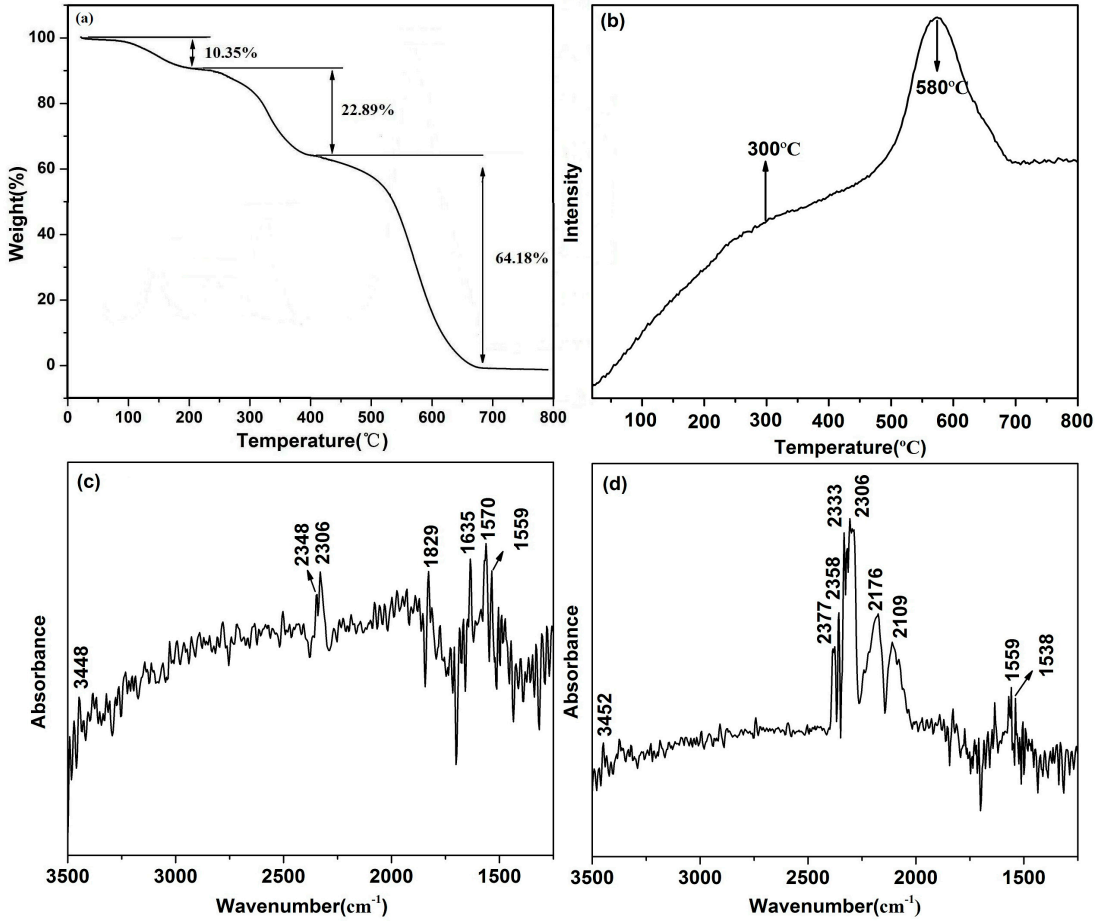

Figure 6. (**a**) TG curve of C_{60}-GAP under air atmosphere; (**b**) IR absorption intensity of the gas released from C_{60}-GAP by time diversification; FTIR spectra of the gaseous product released by C_{60}-GAP at decomposition temperatures of (**c**) 300 °C, and (**d**) 580 °C.

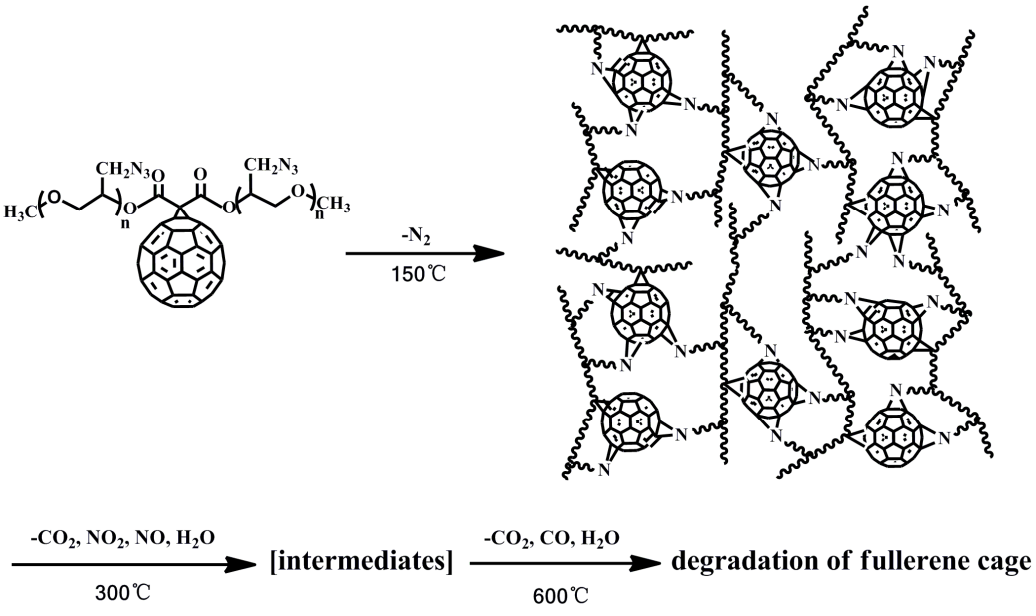

Scheme 2. Thermal decomposition mechanism of C_{60}-GAP under air atmosphere.

To prove the previous assumption, *in situ* FTIR was used to rapidly identify the constituents of decomposition condensed-phase residue. Figure 7a shows the IR spectra of C_{60}-GAP decomposition condensed-phase residue at 27 °C, 106 °C, 124 °C, 149 °C, 172 °C, 205 °C, 261 °C, and 305 °C under air atmosphere. Figure 7b shows the IR absorption intensity ratio of $-N_3$ (υ = 2098 cm^{-1}) and C=O (υ = 1735 cm^{-1}), as well as that of C_{60} (υ = 525 cm^{-1}) and C=O (υ = 1735 cm^{-1}), in C_{60}-GAP decomposition condensed-phase FTIR spectra at specified temperatures. The IR absorption intensity ratio of $-N_3$ (υ = 2098 cm^{-1}) and C=O (υ = 1735 cm^{-1}) ($A_{-N3}/A_{C=O}$), as well as that of C_{60} (υ = 525 cm^{-1}) and C=O (υ = 1735 cm^{-1}) ($A_{C60}/A_{C=O}$), rapidly decreased at 150 °C. The decrease in $A_{-N3}/A_{C=O}$ shows that the $-N_3$ started rapid decomposition at 150 °C, and the reduction in $A_{C60}/A_{C=O}$ at 150 °C indicates that the decomposition of the $-N_3$ group is accompanied with the damage of fullerene conjugated structure. Thus, the TGA-IR and *in situ* FTIR analytical results strictly corroborate that C_{60}-GAP decomposition at 150 °C is through the initial intramolecular or intermolecular reaction of $-N_3$ and the fullerene carbon cage.

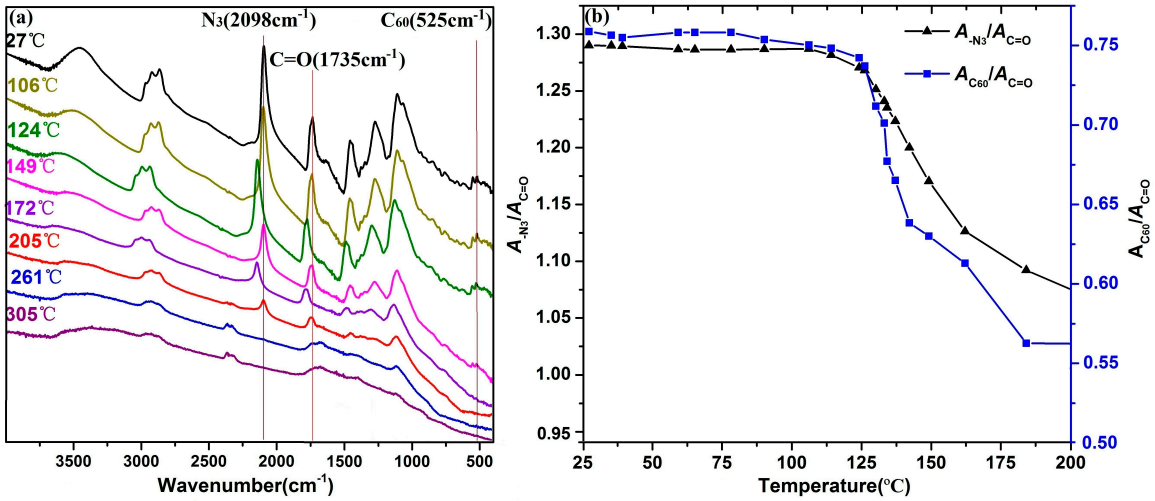

Figure 7. (**a**) FTIR spectra of C_{60}-GAP decomposition condensed-phase at different temperatures under air atmosphere; (**b**) Plots of the IR absorption intensity ratio of $-N_3$ (υ = 2098 cm^{-1}) and C=O (υ = 1735 cm^{-1}), C_{60} (υ = 525 cm^{-1}) and C=O (υ = 1735 cm^{-1}) in C_{60}-GAP decomposition condensed-phase FTIR spectra at different temperatures under air atmosphere.

4. Conclusions

A new energetic polymer fullerene derivative, C_{60}-GAP, has been successfully synthesized by BM-GAP and C_{60}. Its structure was systematically characterized by FTIR, UV-vis, and ^{1}H and ^{13}C NMR spectroscopy analyses. The thermal decomposition mechanism of C_{60}-GAP was analyzed by DSC, TGA-FTIR, and *in situ* FTIR. The results showed that the initial decomposition of C_{60}-GAP at 150 °C could be ascribed to the intramolecular or intermolecular reaction of the $-N_3$ group and fullerene carbon cage. The second thermal degradation at about 200~400 °C is probably due to the decomposition of the GAP main chain and *N*-heterocyclic decomposition. And the last step is maybe because of the thermal decomposition of carbon cage.

Acknowledgments

We are grateful for financial support from the National Natural Science Foundation of China (Project No. 21301142, 51372211), National Defense Fundamental Research Projects (Project No. A3120133002), Youth Innovation Research Team of Sichuan for Carbon Nanomaterials (2011JTD0017), Applied Basic Research Program of Sichuan Province (2014JY0170) and Southwest University of Science and Technology Researching Project (13zx9107, 13zxfk09).

Author Contributions

All listed authors contributed to the research work. Bo Jin conceived and directed the research, Ting Huang conducted, analyzed and interpreted the data. Congdi Chen and Rongzong Zheng analyzed the data. Bo Jin and Rufang Peng proposed idea for explanation, reviewed and approved the manuscript. Yi He and Shijin Chu reviewed the manuscript.

Conflicts of Interest

The authors declare no conflict of interest.

References

1. Hirsch, A. *The Chemistry of the Fullerenes*; Thieme Medical Publishers: Stuttgart, Germany, 1994.
2. Dresselhaus, M.S.; Dresselhaus, G.; Eklund, P.C. *Science of Fullerenes and Carbon Nanotubes: Their Properties and Applications*; Academic Press: Waltham, MA, USA, 1996.
3. Astefanei, A.; Nunez, O.; Galceran, M.T. Analysis of C_{60}-fullerene derivatives and pristine fullerenes in environmental samples by ultrahigh performance liquid chromatography-atmospheric pressure photoionization-mass spectrometry. *J. Chromatogr. A* **2014**, *1365*, 61–71.
4. Butts, C.P.; Jazdzyk, M. The preparation and structures of non-hydrocarbon functionalized fullerene-diamine adducts. *Chem. Commun.* **2003**, *13*, 1530–1531.
5. Chaves, C.W.; Moraes, D.E. Single or functionalized fullerenes interacting with heme group. *AIP Adv.* **2014**, *9*, 097119.
6. Tzirakis, M.D.; Orfanopoulos, M. Radical reactions of fullerenes: from synthetic organic chemistry to materials science and biology. *Chem. Rev.* **2013**, *7*, 5262–5321.
7. Han, X.; Wang, T.F.; Lin, Z.K.; Han, D.L.; Li, S.F.; Zhao, F.Q. RDX/AP-CMDB propellants containing fullerenes and carbon black additives. *Defence Sci. J.* **2009**, *3*, 284–293.
8. Jin, B.; Peng, R.F.; Zhao, F.Q.; Yi, J.H.; Xu, S.Y.; Wang, S.B.; Chu, S.J. Combustion effects of nitrofulleropyrrolidine on RDX-CMDB propellants. *Propellants Explos. Pyrotech.* **2014**, *39*, 874–880.
9. Chiang, L.Y.; Bhonsle, J.B.; Wang, L.; Shu, S.F.; Chang, T.M.; Hwu, J.R. Efficient one-flask synthesis of water-soluble [60]fullerenols. *Tetrahedron* **1996**, *14*, 4936–4972.
10. Hamwi, A.; Marchand, V. Oxidized fullerene derivatives containing hydroxyl, nitro and fluorine groups. *Fullerene Sci. Technol.* **1996**, *5*, 835–851.
11. Franco, J.U.; Ell, J.R.; Hilton, A.K.; Hammons, J.C.; Olmstead, M.M. $C_{60}Cl_6$, $C_{60}Br_8$ and $C_{60}(NO_2)_6$ as selective tools in organic synthesis. *Fuller. Nanotub. Carbon Nanostruct.* **2009**, *4*, 349–360.

12. Cataldo, F. Preparation of polynitrofullerene by the action of dinitrogen tetroxide on C_{60}. *Fullerene Sci. Technol.* **1997**, *1*, 257–265.
13. Franco, C.; Ornella, U.; Giancarlo, A. Synthesis and explosive decomposition of polynitro[60]fullerene. *Carbon* **2013**, *62*, 413–421.
14. Zhai, R.S.; Arindam, D.; Chien, K.H.; Chau, C.H.; Taizoon, C.; Long, Y.C. Polymeric fullerene oxide films produced by decomposition of hexanitro[60]fullerene. *Carbon* **2004**, *2*, 395–403.
15. Kumari, D.; Singh, H.; Patil, M.; Thiel, W.; Pant, C.S.; Banerjee, S. Synthesis, characterization, thermal and computational studies of novel tetra-azido esters as energetic plasticizers. *Thermochim. Acta* **2013**, *562*, 96–104.
16. Lee, D.H.; Kim, K.T.; Jung, H.; Kim, S.H.; Park, S.; Jeon, H.B.; Paik, H.; Min, B.S.; Kin, W. Characterization of 1,2,3-triazole crosslinked polymers based on azide chain-ends prepolymers and a dipolarophile curing agent as propellant binders: The effect of a plasticizer. *J. Taiwan Inst. Chem. Eng.* **2014**, *6*, 3110–3116.
17. Min, B.S.; Kim, C.K.; Ryoo, M.S.; Kim, S.Y. Azide-bearing polymer-based solid composite propellant prepared by a dual curing system consisting of a urethane-forming reaction and a dipolar addition reaction. *Fuel* **2014**, *15*, 165–171.
18. Ding, Y.Z.; Hu, C.; Guo, X.; Che, Y.Y.; Huang, J. Structure and mechanical properties of novel composites based on glycidyl azide polymer and propargyl-terminated polybutadiene as potential binder of solid propellant. *J. Appl. Polym. Sci.* **2014**, *7*, 40007.
19. Huang, T.; Jin, B.; Peng, R.F.; Chu, S.J. Synthesis and characterization of a new energetic plasticizer: Acyl-terminated GAP. *Int. J. Polym. Anal. Charact.* **2014**, *6*, 522–531.
20. Jin, B.; Dong, H.S.; Peng, R.F.; Shen, J.; Tan, B.S.; Chu, S.J. Synthesis and characterization of poly(vinyl 2,4,6-trinitrophenylacetal) as a new energetic binder. *J. Appl. Polym. Sci.* **2011**, *3*, 1643–1648.
21. Frankel, M.B.; Grant, L.R.; Flanagan, J.E. Historical development of glycidyl azide polymer. *J. Propuls. Power* **1992**, *3*, 560–563.
22. Kim, E.S.; Yang, V.; Lian, Y.C. Modeling of HMX/GAP pseudo-propellant combustion. *Combust. Flame* **2002**, *3*, 227–245.
23. Hu, C.; Guo, X.; Jing, Y.; Chen, J.; Zhang, C.; Huang, J. Structure and mechanical properties of crosslinked glycidyl azide polymers via click chemistry as potential binder of solid propellant. *J. Appl. Polym. Sci.* **2014**, *16*, 40636.
24. Li, N.; Xiong, X.F.; Mo, H.C.; Lu, X.M.; Liu, Y.J. Synthesis and properties of azide terminated and acetate terminated glycidyl azide polymer. *J. Solid Rocket Technol.* **2013**, *2*, 234–236.
25. Jin, B.; Shen, J.; Peng, R.F.; Zheng, R.Z.; Chu, S.J. Efficient cyclopropanation of [60]fullerene starting from bromo-substituted active methylene compounds without using a basic catalyst. *Tetrahedron Lett.* **2014**, *36*, 5007–5010.
26. Guerra, S.; Trinh, T.M.N.; Schillinger, F.; Muhlberger, L.; Sigwalt, D.; Holler, M. The di-*t*-butylsilylene protecting group as a bridging unit in linear and macrocyclic bis-malonates for the regioselective multifunctionalization of C_{60}. *Tetrahedron Lett.* **2013**, *46*, 6251–6257.
27. Zhao, Y.B.; Luo, Y.J.; Li, X.M. Synthesis and characterization of BAMO-r-GAP copolymer. *Polym. Mater. Sci. Eng.* **2012**, *9*, 1–4.

28. Mohan, Y.M.; Raju, K.M. Synthesis and characterization of low molecular weight azido polymers as high energetic plasticizers. *Int. J. Polym. Anal. Charact.* **2004**, *5–6*, 289–304.
29. Sigwalt, D.; Schillinger, F.; Guerra, S.; Holler, M.; Berville, M.; Nierengarten, J.F. An expeditious regioselective synthesis of [60]fullerene e,e,e tris-adduct building blocks. *Tetrahedron Lett.* **2013**, *32*, 4241–4244.
30. Shirosaki, T.; Harisaki, R.; Horikawa, M.; Sakurai, H.; Nagaoka, S.; Ihara, H. Synthesis of a series of malonic diester-introduced fullerene derivatives. *Synth. Commun.* **2014**, *2*, 275–279.
31. Wang, G.W.; Li, J.X.; Xu, Y. Synthesis of C_{60}-fused tetrahydrothiophene derivatives via nucleophilic cycloaddition of thiocyanates. *Org. Biomol. Chem.* **2008**, *16*, 2995–2999.
32. Li, F.B.; You, X.; Wang, G.W. Synthesis of disubstituted [60]fullerene-fused lactones: Ferric perchlorate promoted reaction of [60]fullerene with malonate esters. *Org. Lett.* **2010**, *21*, 4896–4899.
33. Zhang, L.Y.; Liu, Z.R.; Wang, X.H.; Heng, S.Y.; Pan, Q.; Zhao, F.Q. Investigation on thermal decomposition of GAP by FTIR spectroanalysis. *J. Solid Rocket Technol.* **2010**, *5*, 549–553.
34. Korobeinichev, O.P.; Kuibida, L.V.; Volkov, E.N.; Shmakov, A.G. Mass spectrometric study of combustion and thermal decomposition of GAP. *Combust. Flame* **2002**, *1*, 136–150.
35. Sun, Y.; Li, S. The effect of nitrate esters on the thermal decomposition mechanism of GAP. *J. Hhazard. Mater.* **2008**, *1*, 112–117.
36. Kay, K.Y.; Han, K.J.; Yu, Y.J.; Park, Y.D. Dendritic fullerenes (C_{60}) with photoresponsive azobenzene groups. *Tetrahedron Lett.* **2002**, *29*, 5053–5056.
37. González, S.; Martín, N.; Swartz, A.; Guldi, D.M. Addition reaction of azido-exTTFs to C_{60}: Synthesis of fullerotriazoline and azafulleroid electroactive dyads. *Org. Lett.* **2003**, *4*, 557–560.
38. Fazhoğlu, H.; Hacaloğlu, J. The effect of triethanolamine on thermal decomposition of GAP. *J. Macromol. Sci. A* **2002**, *7*, 759–768.
39. Fazlıoğlu, H.; Hacaloğlu, J. Thermal decomposition of glycidyl azide polymer by direct insertion probe mass spectrometry. *J. Anal. Appl. Pyrolysis* **2002**, *2*, 327–338.
40. Jin, B.; Shen, J.; Peng, R.F.; Shu, Y.J.; Tan, B.S.; Chu, S.J.; Dong, H.S. Synthesis, characterization, thermal stability and sensitivity properties of the new energetic polymer through the azidoacetylation of poly(vinyl alcohol). *Polym. Degrad. Stab.* **2012**, *4*, 473–480.